B(E2) Data From ENSDF Using GTNDSE

W. D. Kulp, J. L. Wood, J. M. Allmond
Georgia Institute of Technology

- Systematics
  - Nuclear structure indicator
  - Evaluation tool
  - Error identification
- Experimental Methods
  - Electronic timing
  - Doppler methods
  - Coulomb excitation
- Compliations
  - Multi-Coulex matrix elements
- Evaluations
  - Multi-Coulex input/output issues
- Nuclear Structure
  - Triaxial rotor model
- Future

Systematics

Collective model

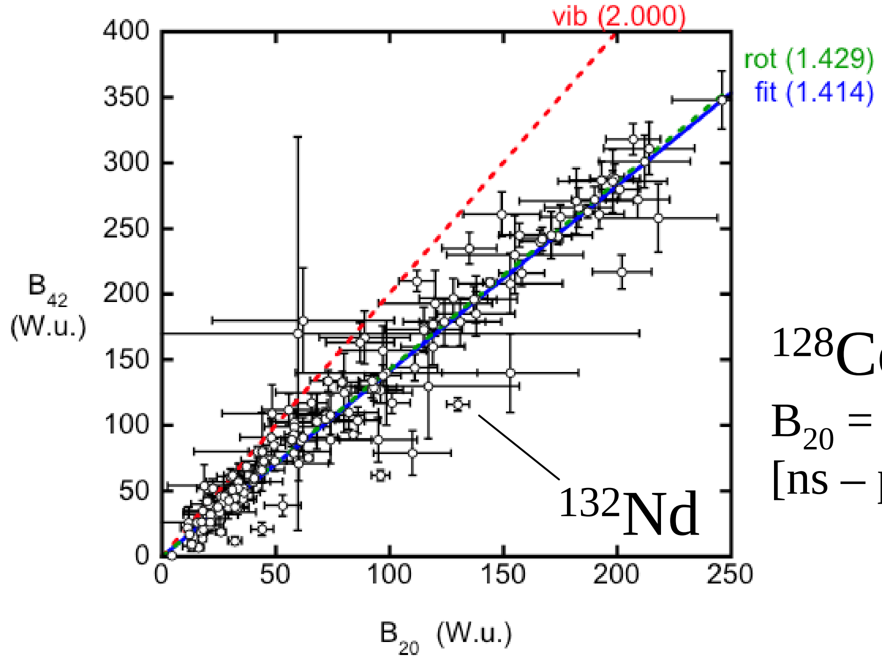

^{128}Ce

B_{20} = 111,000

[ns – ps]

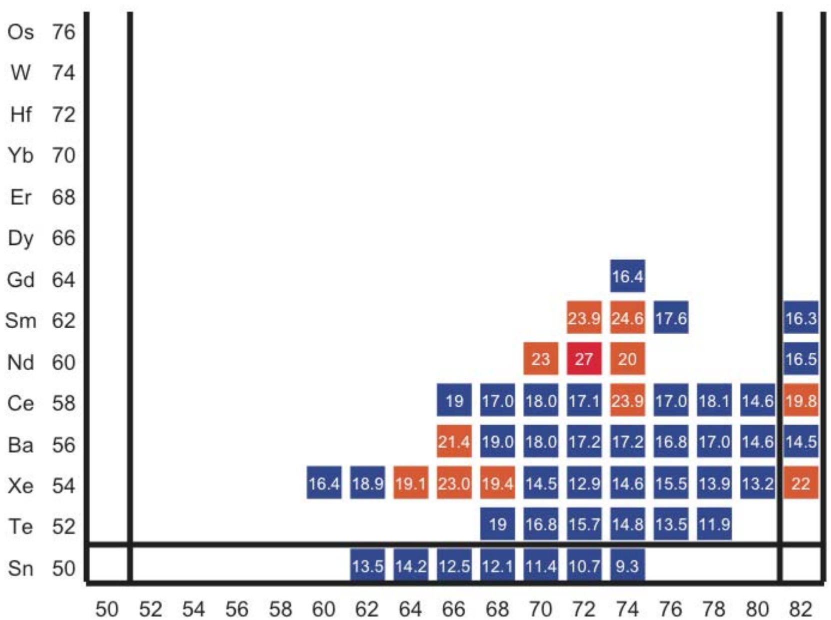

Grodzins relation

$$[E(2_1^+)\ \mathrm{keV}]\ [B(E2)\uparrow e^2\cdot b^2]\ \frac{A}{Z^2}\simeq 16.0$$

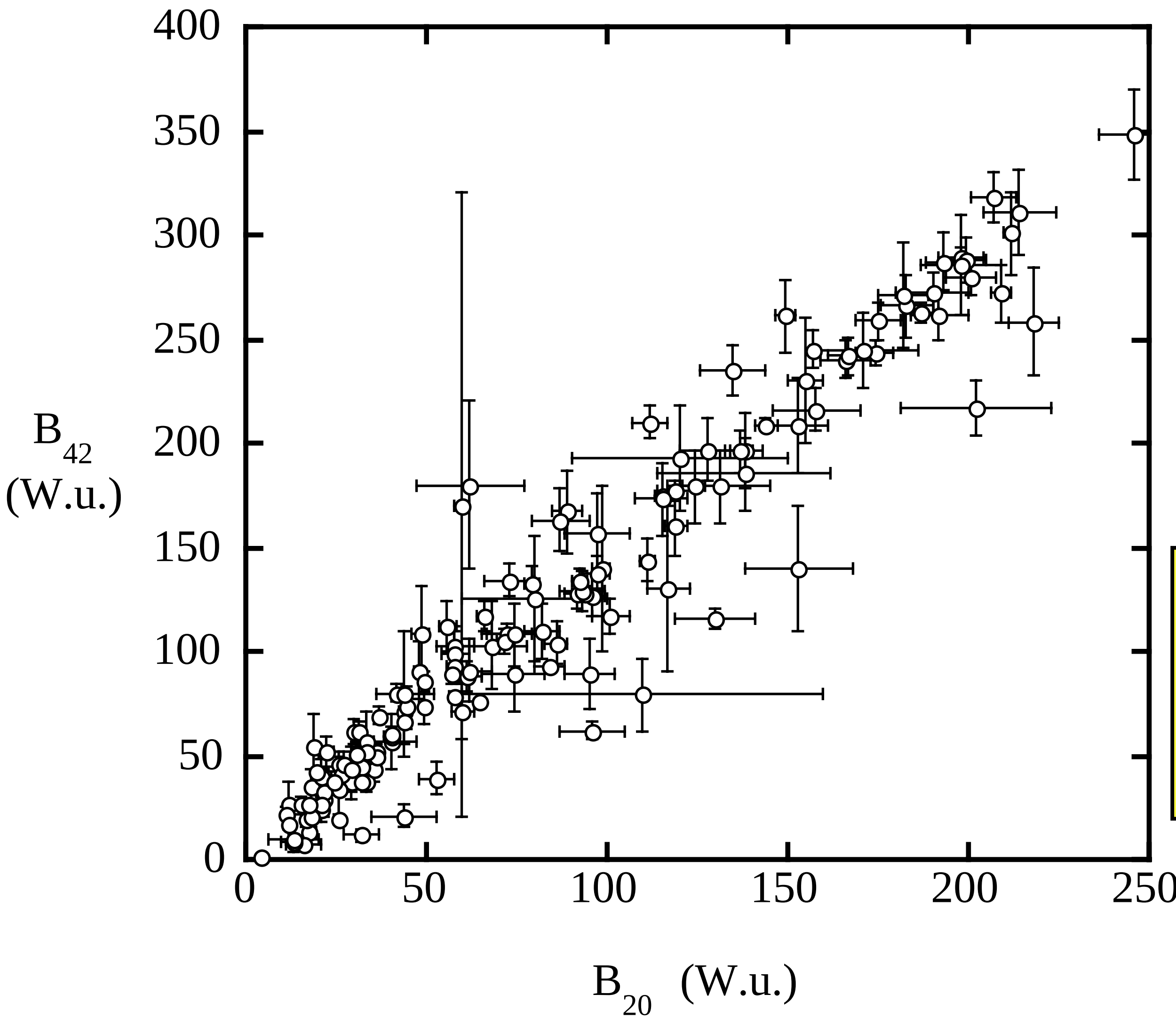

^{128}Ce

B_{20} = 111,000

!

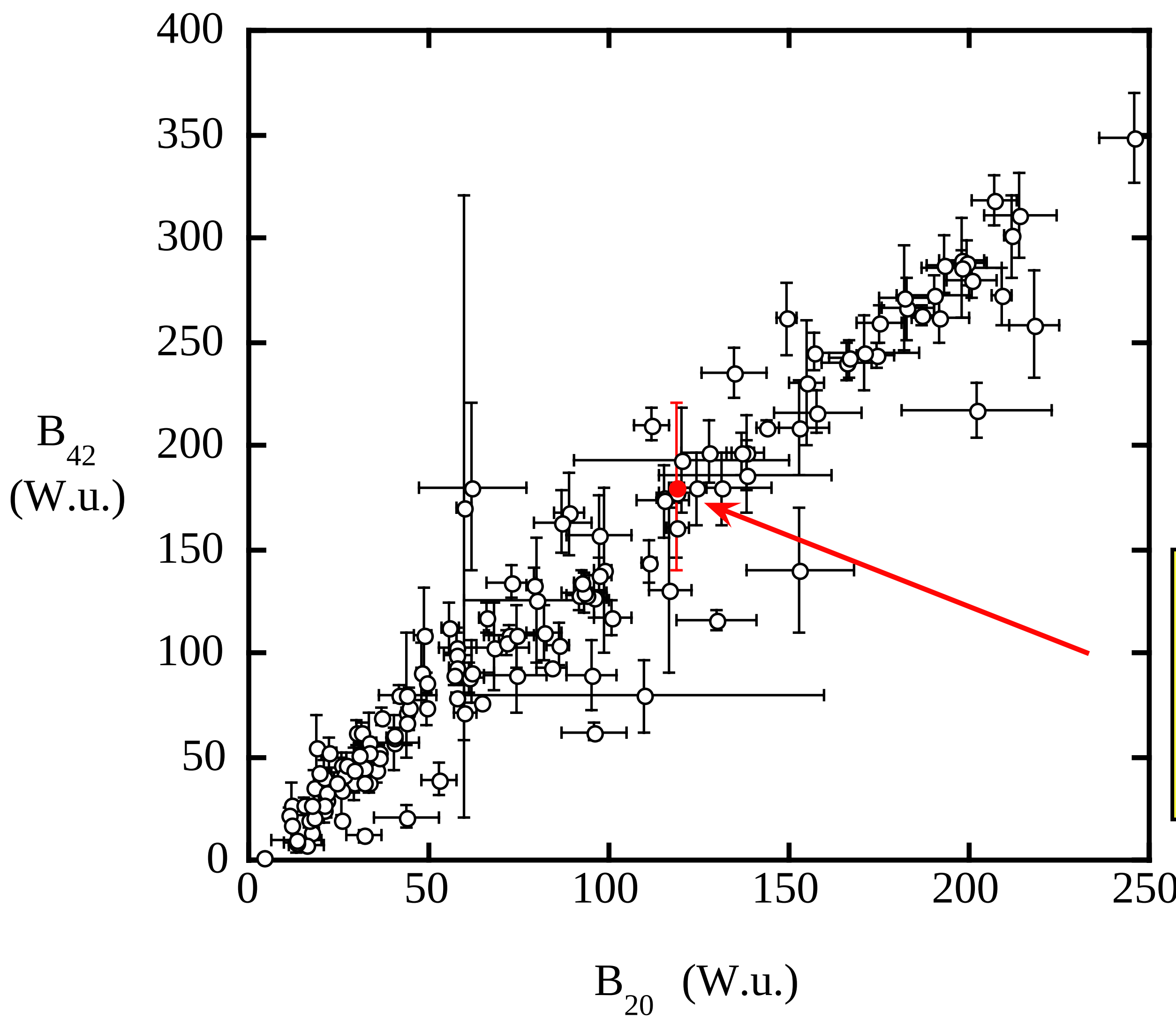

^{128}Ce
B_{20} = 111,000
[ns - ps]

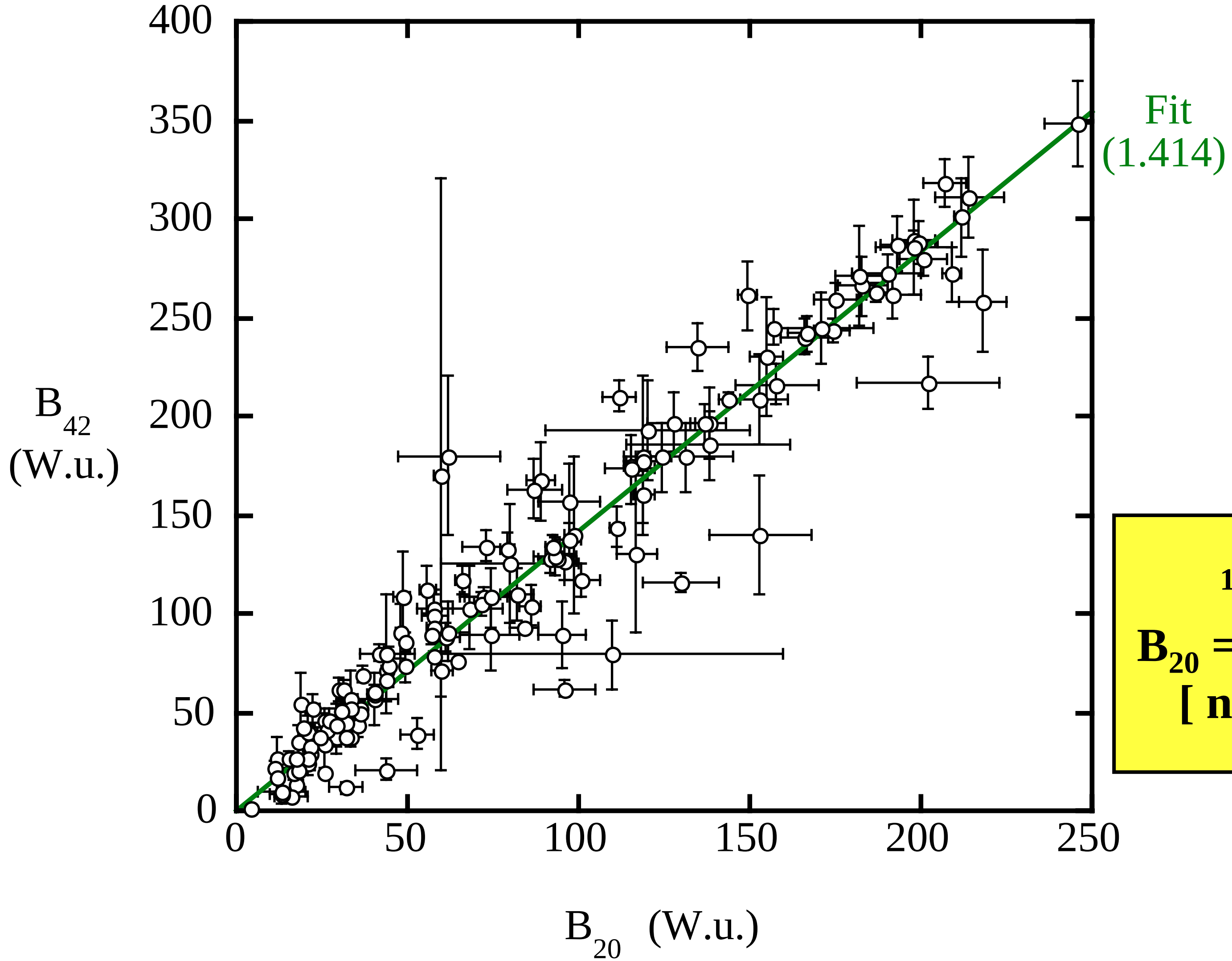

[128]Ce

B_{20} = 111,000

[ns - ps]

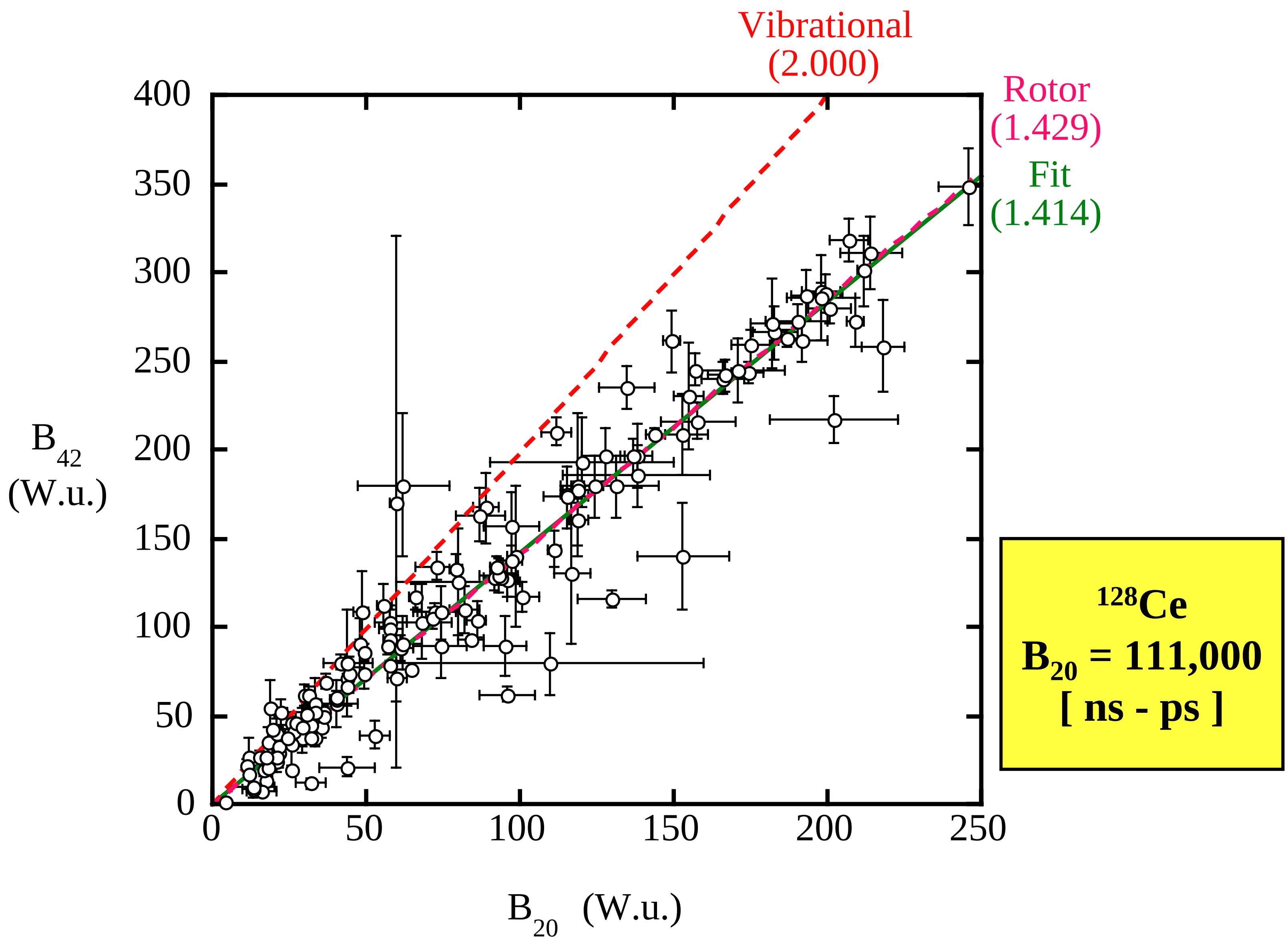

Vibrational
(2.000)
Rotor
(1.429)
Fit
(1.414)
400
350
300
250
200
150
100
50
0
B42
(W.u.)
0
50
100
150
200
250
B20 (W.u.)
128Ce
B20 = 111,000
[ns - ps]

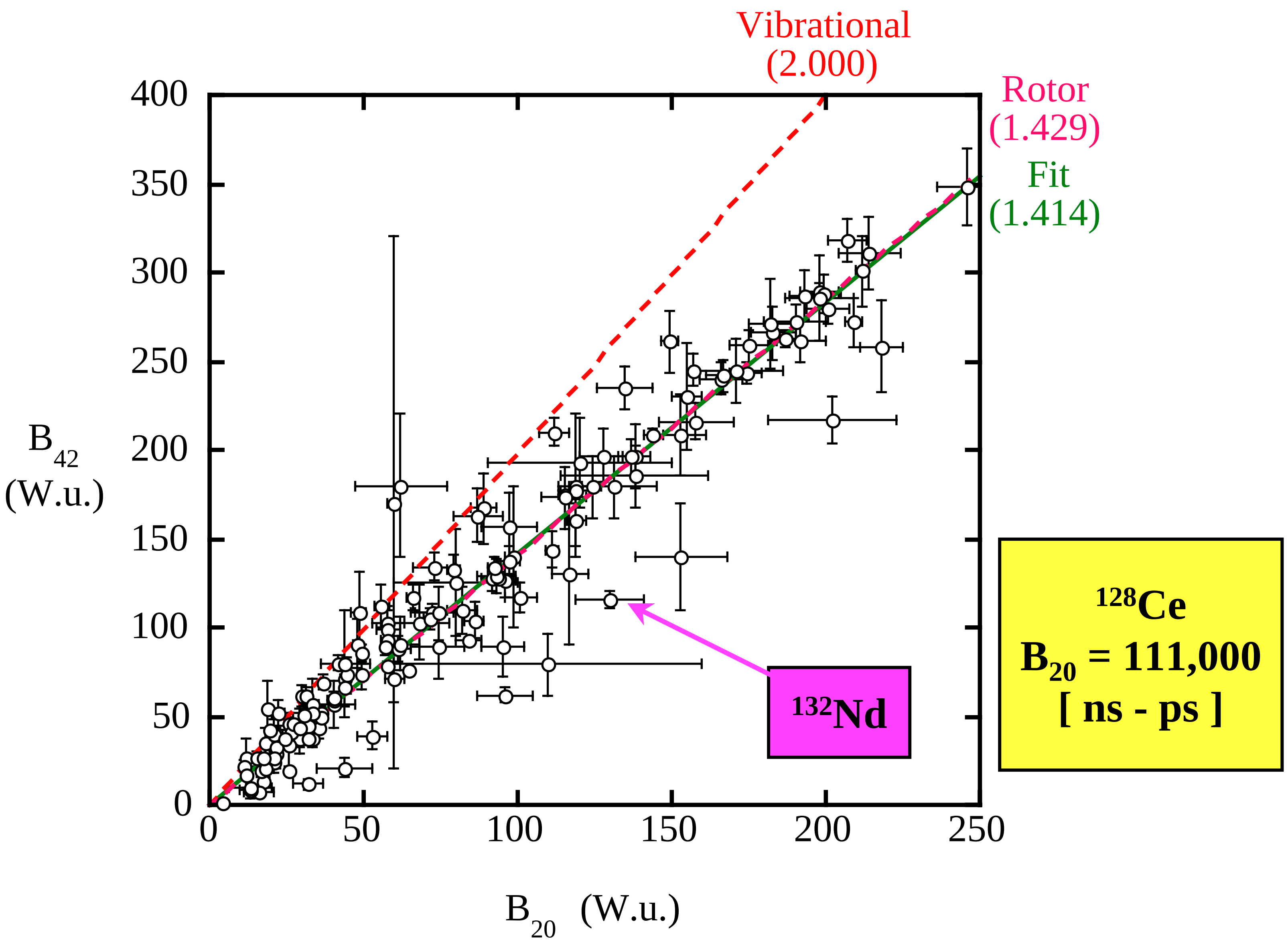

Vibrational
(2.000)
Rotor
(1.429)
Fit
(1.414)
400
350
300
250
200
150
100
50
0
B42
(W.u.)
0
50
100
150
200
250
B20 (W.u.)
132Nd
128Ce
B20 = 111,000
[ns - ps]

Ref.	$T_{1/2}$ (2^+_1) ps	B(E2) Wu	Grodzins
1986Ma39	220^{20}	128	20.0
1987Wa02	243^{21}	116	18.1
1989Mo10	186^{13}	152	23.8
1995Ma96	133^{8}	212	33.1
NDS	216^{17}	130	20.3
Raman01	166^{28}	174	27.2

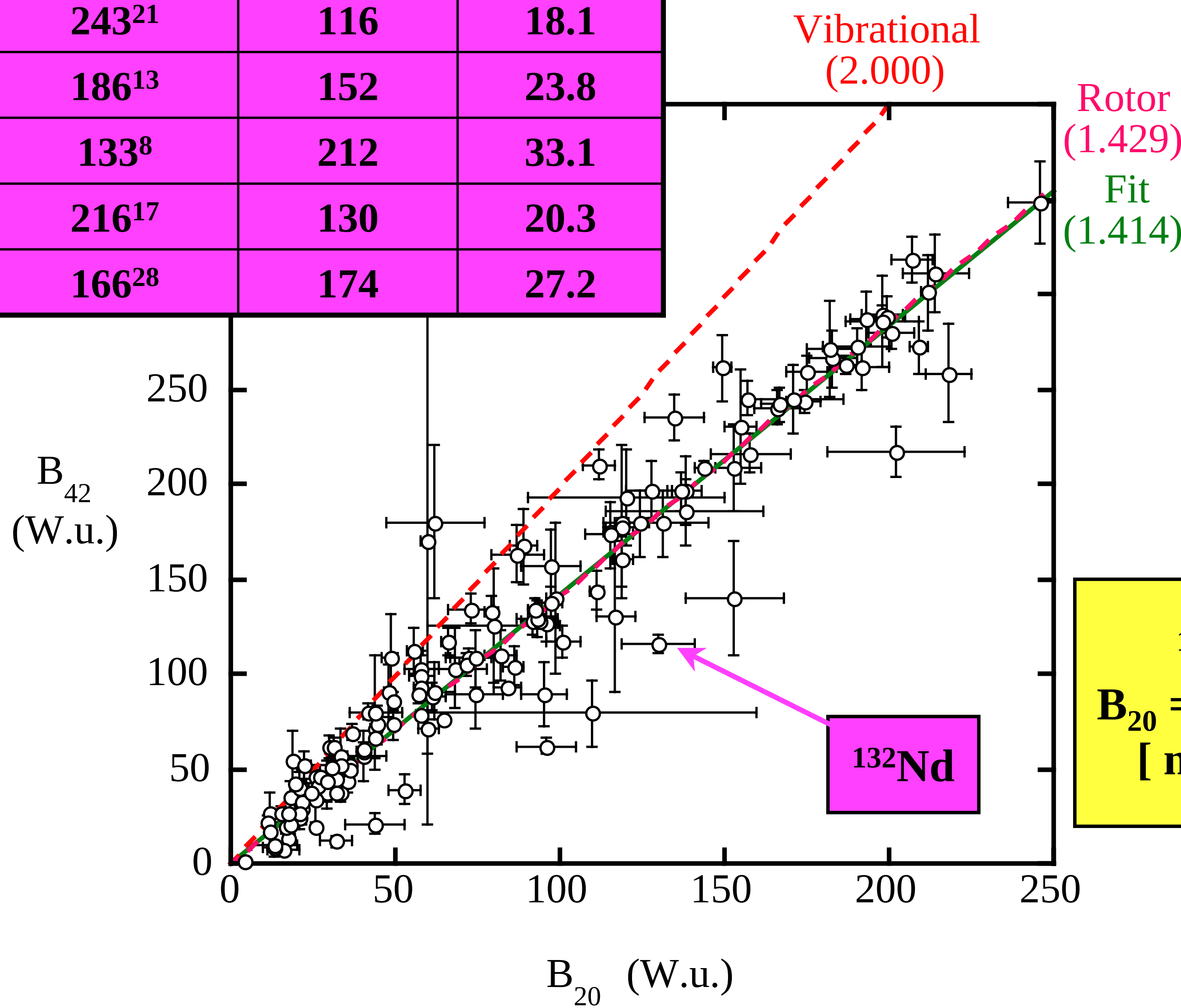

^{128}Ce

B_{20} = 111,000

[ns - ps]

Grodzins rule

$$\left[E(2_1^+)\ \mathrm{keV}\right]\left[B(E2)\uparrow e^2\cdot b^2\right]\frac{A}{Z^2}\simeq 16.0$$

		50	52	54	56	58	60	62	64	66	68	70	72	74	76	78	80	82
Os	76																	
W	74																	
Hf	72																	
Yb	70																	
Er	68																	
Dy	66																	
Gd	64													16.4				
Sm	62												23.9	24.6	17.6			16.3
Nd	60											23	27	20				16.5
Ce	58									19	17.0	18.0	17.1	23.9	17.0	18.1	14.6	19.8
Ba	56									21.4	19.0	18.0	17.2	17.2	16.8	17.0	14.6	14.5
Xe	54						16.4	18.9	19.1	23.0	19.4	14.5	12.9	14.6	15.5	13.9	13.2	22
Te	52										19	16.8	15.7	14.8	13.5	11.9		
Sn	50							13.5	14.2	12.5	12.1	11.4	10.7	9.3				

Experimental methods

- **Electronic timing methods**
  - Delay
  - Centroid shift in time spectrum
- **Doppler methods**
  - DSAM

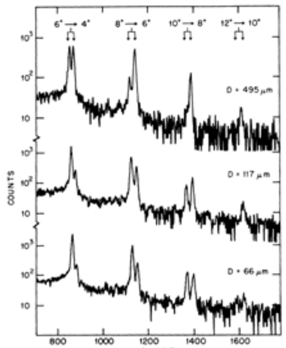

FIG. 1. γ-ray spectra for different target-stopper separations taken with a Ge(Li) γ-ray detector. Excitation was produced by a 153-MeV ^{40}Ar beam on the ^{236}U target.

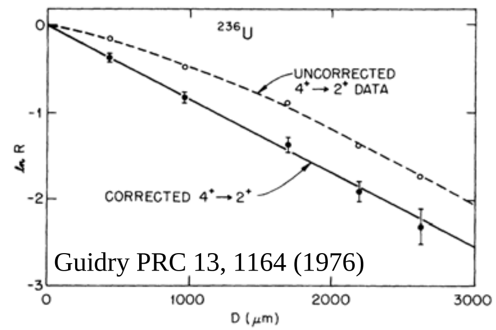

Guidry PRC 13, 1164 (1976)

FIG. 3. Ln*R* vs *D* for the $4^+ \to 2^+$ transition in the ^{236}U ground band. The open circles represent experimental data, while closed points represent the corrected data from which the lifetime is extracted.

- (n,n'γ)

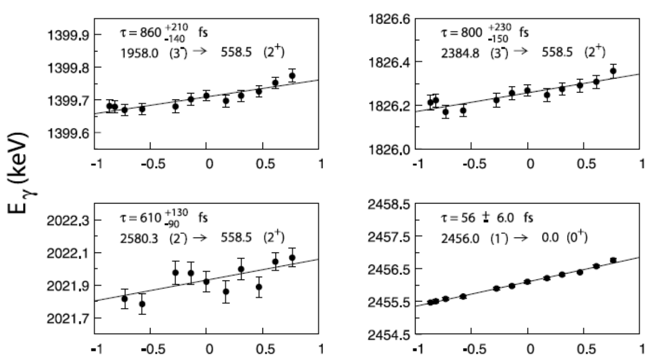

Bandyopadhyay PRC 68, 014324 (2003)

cos θ

FIG. 2. γ-ray energies as a function of cos θ for the indicated transitions. The lines are linear fits to the data from which the $F(\tau)$ values have been extracted.

- **Coulomb Excitation**
  - Multiple-step
  - Radioactive beams
- DBLS

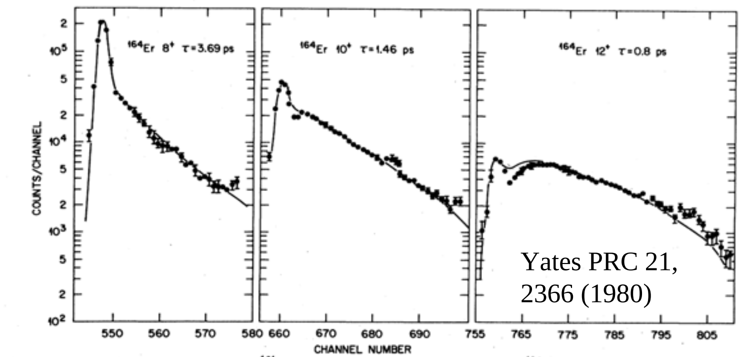

Yates PRC 21, 2366 (1980)

FIG. 9. Line-shape fits to transitions in ^{164}Er following excitation by 620-MeV ^{136}Xe ions. The points are the experimental data and the solid lines are the calculated fits from the program DOPCO (Ref. 23).

- GRID

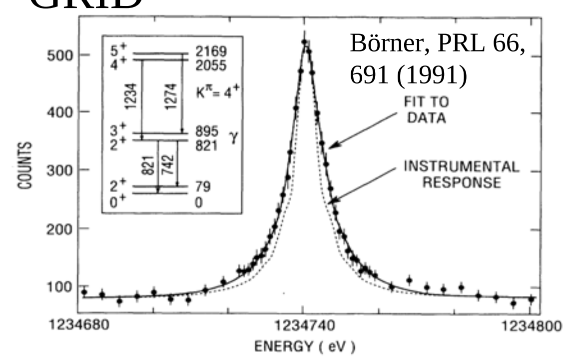

Börner, PRL 66, 691 (1991)

FIG. 1. Measured profile of the 1234-keV transition from a summation of ten individual scans. The solid-line fit to the data uses the Bethe formula for the extraction of the recoil velocities (τ = 440 fs). The dashed-line profile is the measured instrumental response function. Inset: Part of the ^{168}Er decay scheme.

DSAM

Doppler-shift attenuation method

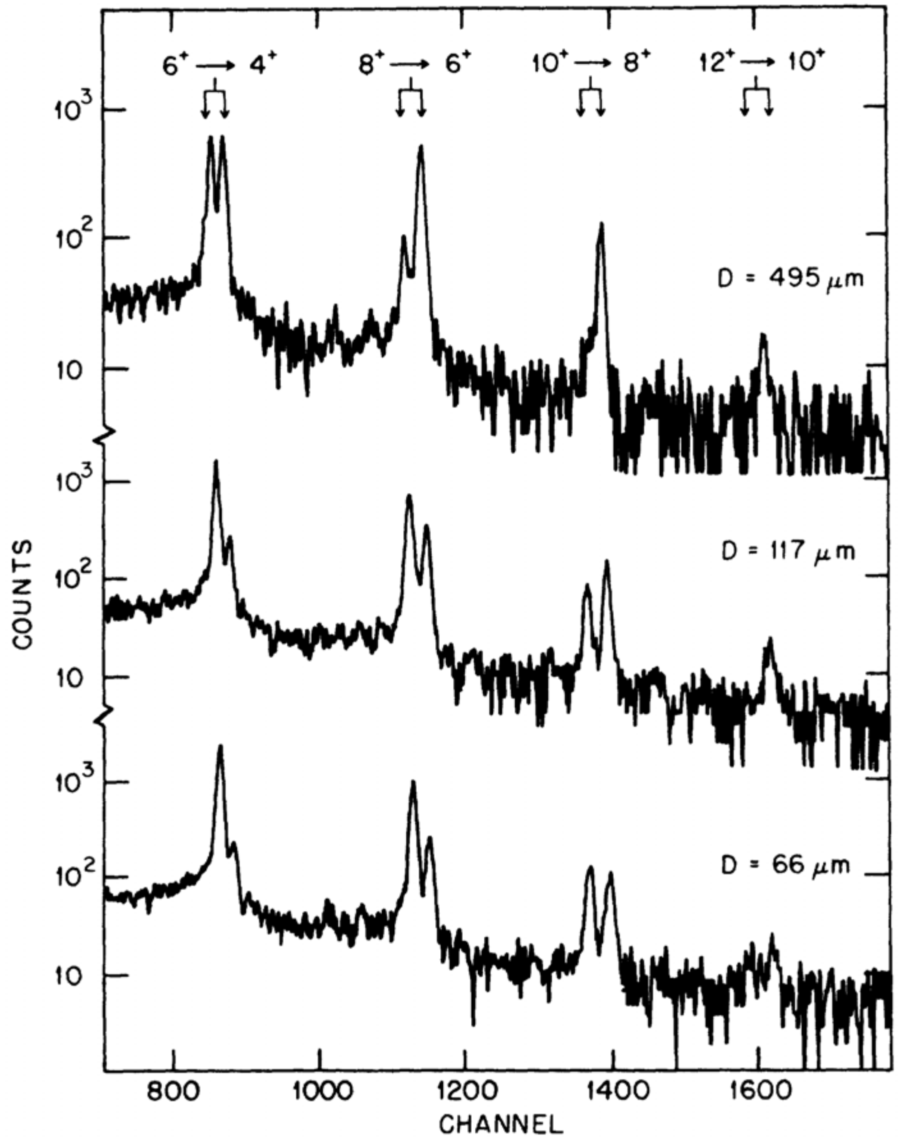

FIG. 1. γ-ray spectra for different target-stopper separations taken with a Ge(Li) γ-ray detector. Excitation was produced by a 153-MeV ^{40}Ar beam on the ^{236}U target.

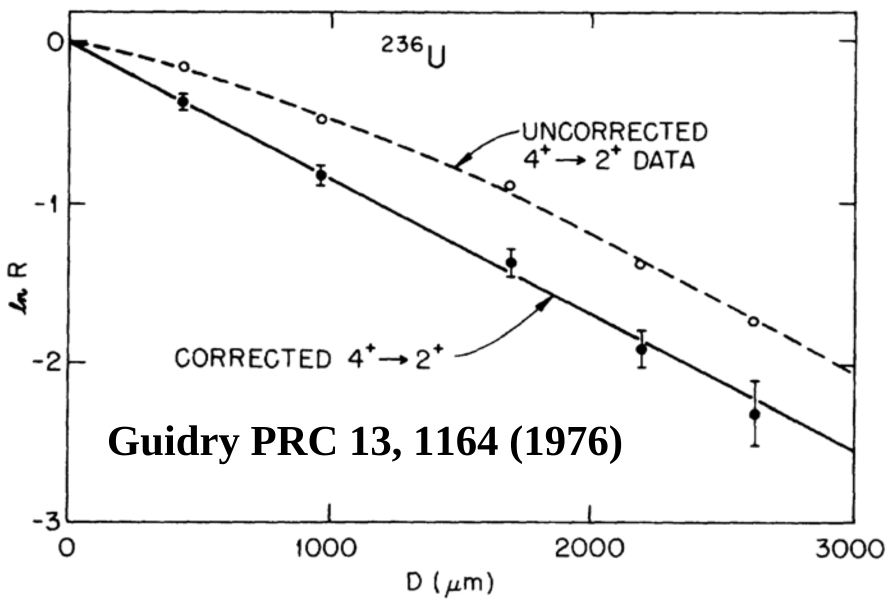

FIG. 3. LnR vs D for the $4^+ \to 2^+$ transition in the ^{236}U ground band. The open circles represent experimental data, while closed points represent the corrected data from which the lifetime is extracted.

(n,n’γ)

inelastic neutron scattering

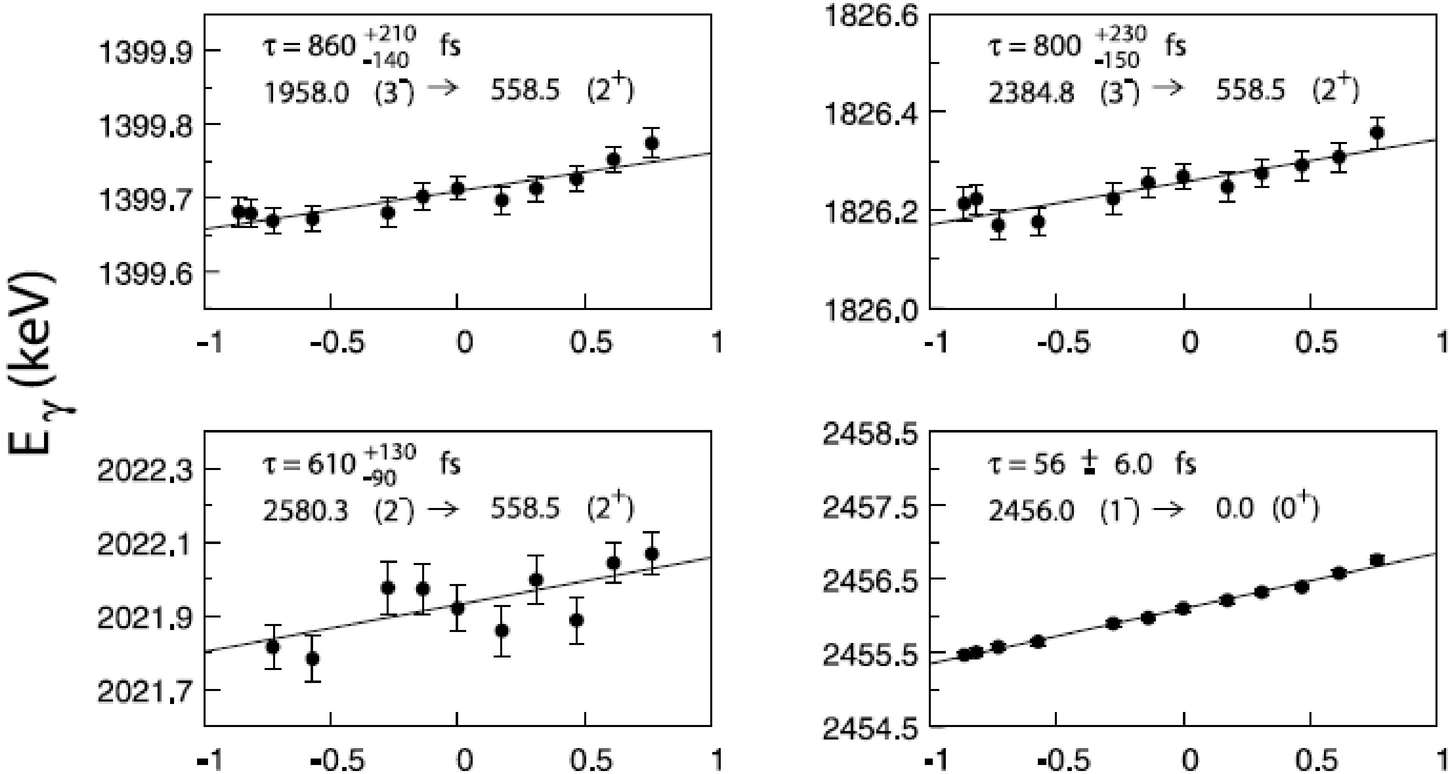

Bandyopadhyay PRC 68, 014324 (2003)

FIG. 2. γ-ray energies as a function of cos θ for the indicated transitions. The lines are linear fits to the data from which the $F(\tau)$ values have been extracted.

DBLS

Doppler-broadened line shape

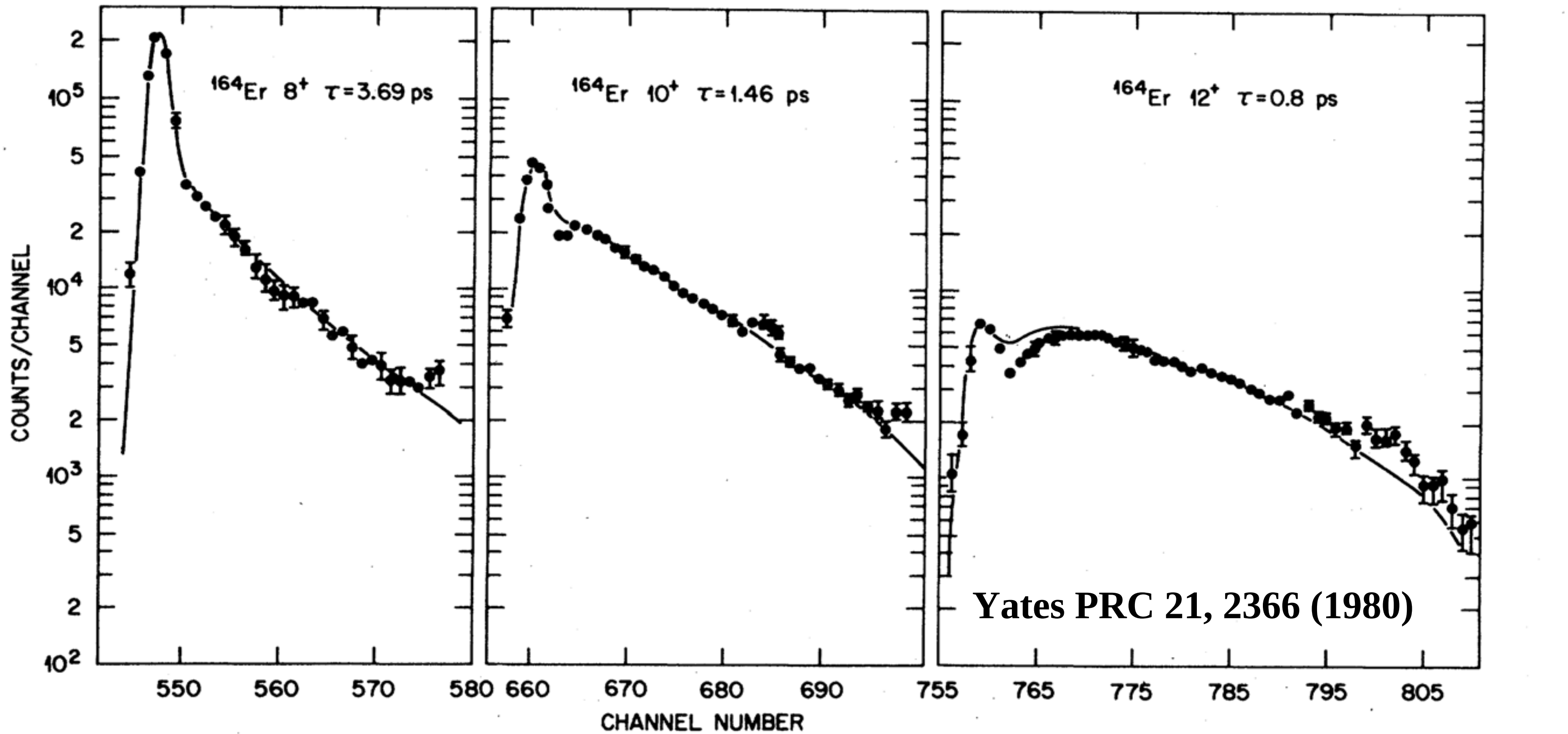

FIG. 9. Line-shape fits to transitions in ^{164}Er following excitation by 620-MeV ^{136}Xe ions. The points are the experimental data and the solid lines are the calculated fits from the program DOPCO (Ref. 23).

GRID

γ-ray-induced Doppler broadening

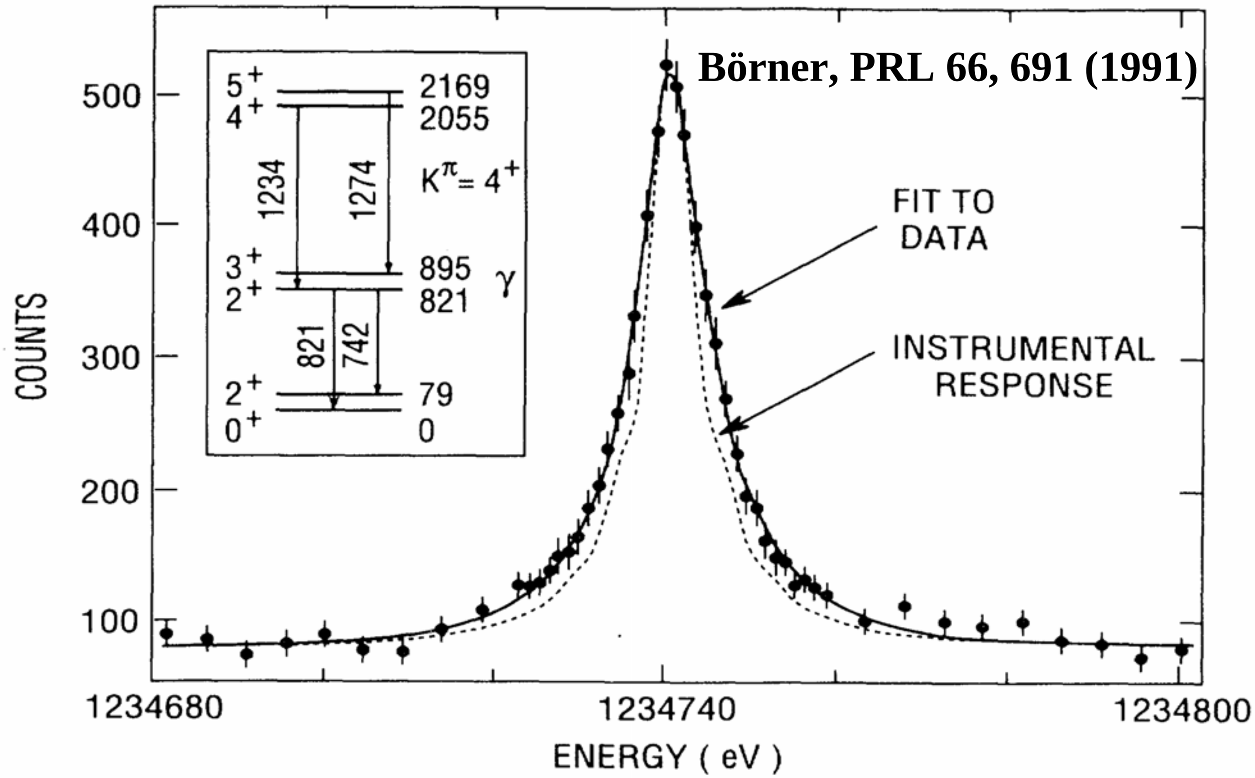

FIG. 1. Measured profile of the 1234-keV transition from a summation of ten individual scans. The solid-line fit to the data uses the Bethe formula for the extraction of the recoil velocities ($\tau = 440$ fs). The dashed-line profile is the measured instrumental response function. Inset: Part of the ^{168}Er decay scheme.

Coulomb excitation

Kulp, unpublished

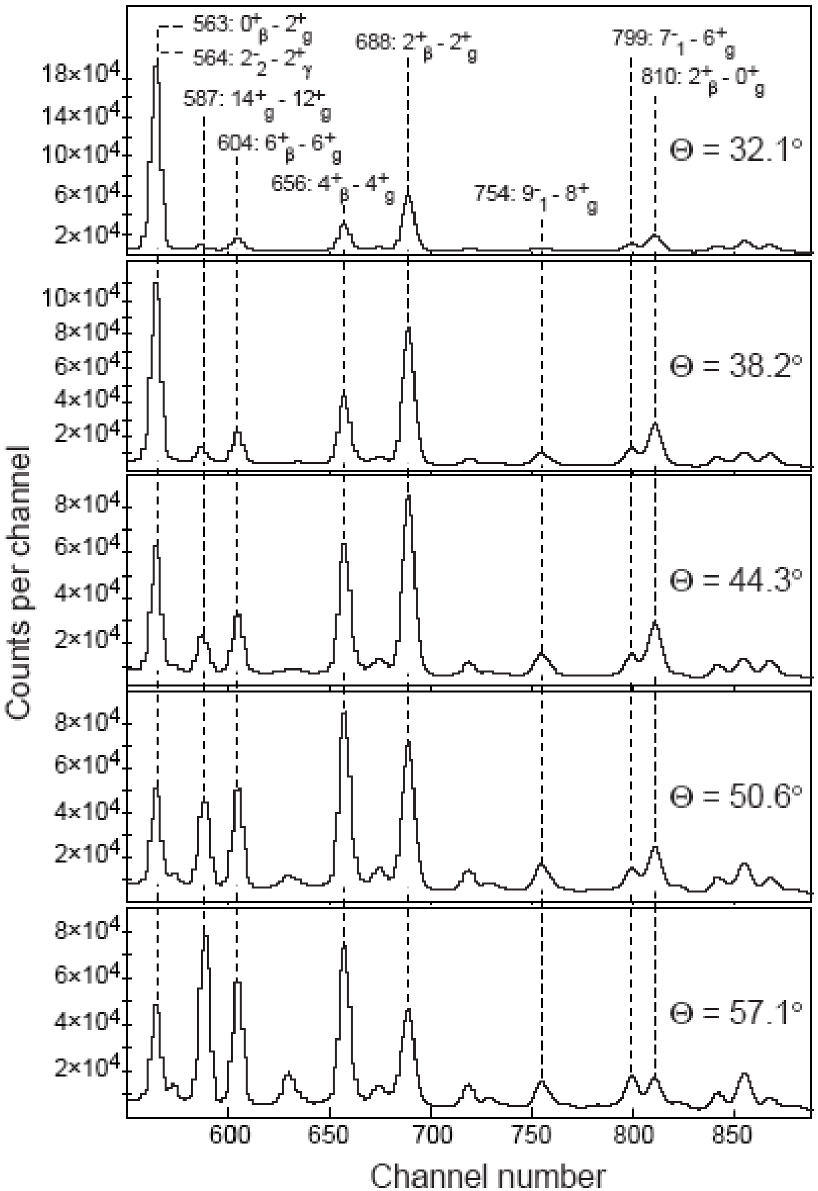

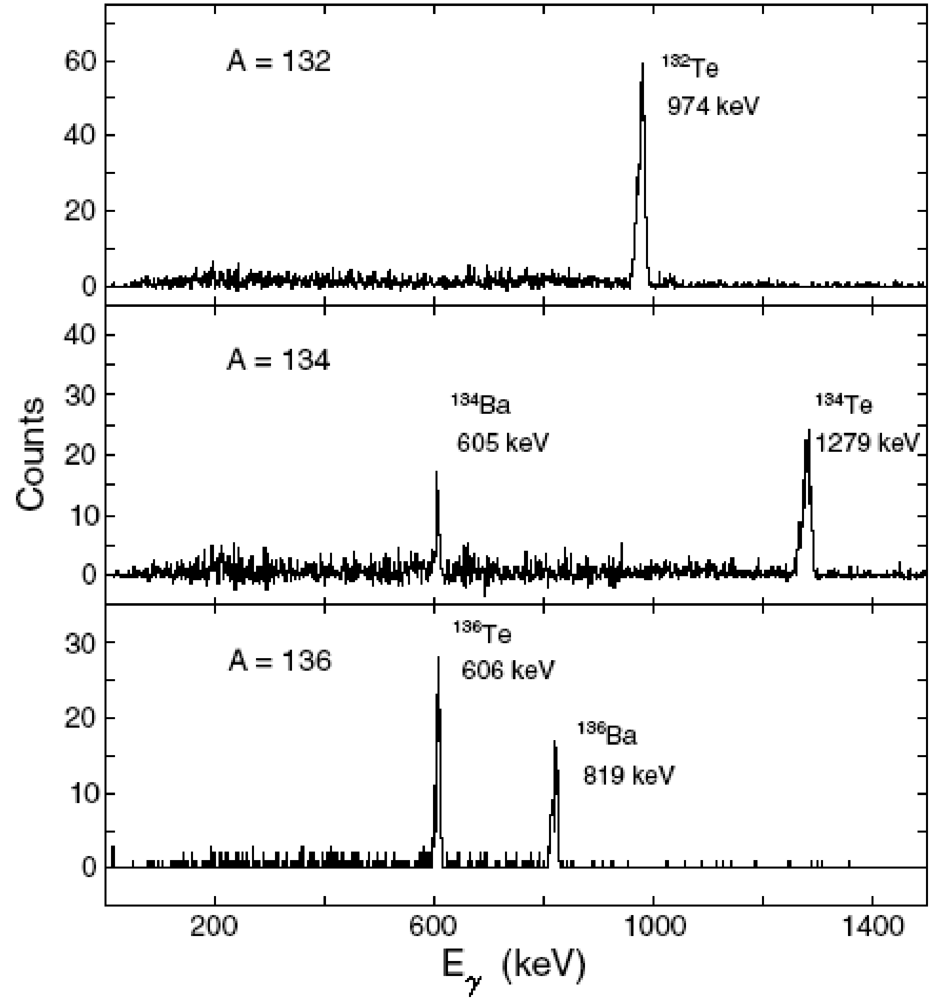

FIG. 1. γ rays from Coulomb excitation of the radioactive ion beams, Doppler-shift corrected and gated by prompt coincidence with carbon recoils in the HyBall detectors. Peaks are all $2_1^+ \rightarrow 0^+$ transitions and are labeled by nuclide and energy.

Radford PRL 88, 0222501 (2002)

- Compilations: multi-Coulex ME’s

$^{66,\,68}$Zn	^{98,100}Mo	^{148,150}Nd	^{182,184}W
^{70,72,74,76}Ge	^{104}Ru	^{156}Gd	^{186,188,190,192}Os
^{76,78,80,82}Se	^{106,108,110}Pd	^{166,168}Er	^{194}Pt
^{82,84}Kr	^{114}Cd	^{172}Yb	

- Evaluations: multi-Coulex input/output issues
  - Input:
    - ME’s from B(σλ)’s; systematics; models
    - Branching ratios
    - Mixing ratios
  - Output: degradation of branching ratios
- Nuclear structure: triaxial rotor model

  “Triaxial rotor model for nuclei with independent inertia and electric quadrupole tensors” Wood, et al., PRC 70, 024308 (2004)

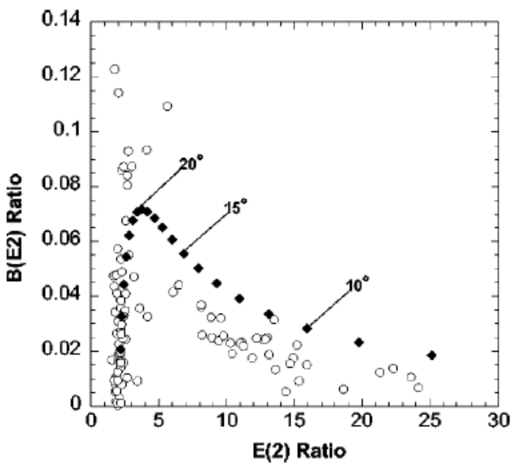

- Future
  - Mini-review of B(E2) data
  - Multi-Coulex ME’s for ENSDF
  - Begin assessment of experimental methods